

Temperature field inversion and break-down at the interface of semi-transparent two-layer system in radiative heat transfer

Boris I. Aronov, Yoram Zvirin *

Faculty of Mechanical Engineering, Technion, Israel Institute of Technology, Haifa, 32000, Israel

(Received 29 June 2000, accepted 3 January 2001)

Abstract—The paper describes analysis of radiation heat transfer in a system of semi-transparent two layers, with a diffuse or partially diffuse interface. Two cases are considered, of “optically closed” and “optically open” systems. In the former case, heater and cooler surfaces with angular-dependent emissivities enclose the two layers. In the latter case, the system is irradiated by a collimated heat flux on one side and the two boundary surfaces radiate to space. Two interesting phenomena have been found from the results obtained by the mathematical-numerical methods developed here: inversion and break-up of the temperature field. In some cases, depending on the radiation properties of the heater and cooler surfaces and on the refraction indices of the layers and the specular–diffuse shares of the interface: the temperature decreases from the side facing the heater to the interface, exhibits a sharp jump increase across it, and then decreases, again, in the second layer (facing the cooler). The whole temperature curve is sometimes higher in the second layer than in the first one. These phenomena occur due to collimation of the radiative heat flux at the boundary surface facing the heater and “de-focusing” the flux at the diffuse (or partially diffuse) interface. The strength of these effects depends on the radiative properties mentioned above and on the optical thickness. Another phenomenon is that of “heat trap” in the case of “optically open” one- or two-layer system, caused by total internal reflection. © 2001 Éditions scientifiques et médicales Elsevier SAS

radiative heat transfer / participating media / semi-transparent layer / diffuse interface

Nomenclature

C	volumetric specific heat . . .	$\text{J} \cdot \text{m}^{-3} \cdot \text{K}^{-1}$	n	refraction index	
F	radiation flux, equations (16) and (17)	$\text{W} \cdot \text{m}^{-2}$	q	net radiation heat flux	$\text{W} \cdot \text{m}^{-2}$
i_λ	spectral radiation intensity . .	$\text{W} \cdot \text{m}^{-2} \cdot \mu\text{m}^{-1} \cdot \text{sr}^{-1}$	Q	difference of radiation fluxes, equation (19)	$\text{W} \cdot \text{m}^{-2}$
I^\pm, I_C^-, I_H^+	integrals over the azimuth angle of the radiation intensities in the \pm directions in the medium, and on the surfaces of the cooler and heater	$\text{W} \cdot \text{m}^{-2} \cdot (\text{sr}^{-1} \cdot 2\pi)$	r_C, r_H	specular reflectivities of cooler and heater surfaces	
J_I^\pm, J_{II}^\pm	normalized I_λ^\pm , integrated over λ , within layers I and II	$\text{W} \cdot \text{m}^{-2}$	$r_{d, \text{mI}}, r_{d, \text{mII}}$	diffuse components of interface reflectivities (at $x = x_m$), on sides facing layers I and II	
K	specular reflection fraction of the interface		$r_{s, \text{mI}}, r_{s, \text{mII}}$	specular components of interface reflectivities (at $x = x_m$), on sides facing layers I and II	
L_I, L_{II}	geometrical thicknesses of the system layers, see figure 1 . .	m	R_{s, m_j}	“purely specular” interface reflectivity on side facing layer j	
M	number of grid points		s_λ	optical thickness for wavelength λ	
			S	optical thickness of the whole two-layer system	
			t	time	
			Δt	time difference (pseudo Δt in iterative process)	s
			T	temperature	K
			ΔT_m	temperature jump at the interface . . .	K

* Correspondence and reprints.

E-mail address: zvirin@tx.technion.ac.il (Y. Zvirin).

x, x_i	distance, x -coordinate of the center of control element i	m
Z_I, Z_{II}	integrals over μ, η of normalized intensities at the interface	$W \cdot m^{-2}$

Greek symbols

α	absorptivity, equal to emissivity	
α_λ	spectral absorption coefficient, equation (4) .	m^{-1}
η	cosine of polar angle of radiation beam in layer II	
θ	polar angle of radiation beam	rad
λ	wavelength	μm
μ	cosine of polar angle of radiation beam in layer I	
Ω	solid angle	sr

Indices

b	black body radiation
C	cooler surface, see figure 1
m	at the interface between the two layers, see figure 1
H	heater surface, see figure 1
s	space
λ	for wavelength λ
I, II	layers I and II, see figure 1

1. INTRODUCTION

Radiation heat transfer in participating media has many important applications and has strong effects in various phenomena, occurring in energy systems and atmospheric processes. Generally, the radiation problems are complicated because they are influenced by many parameters. The properties like reflectivity, absorptivity and transmissivity depend on the wavelength, temperature and material composition. The radiation spectrum depends on both external sources and internal emission. The problems are even more complex when the geometry is not simple and when conduction and/or convection are also involved. Therefore, many theoretical studies have been conducted for problems of pure (or sometimes combined) radiation in planar geometry, in order to gain better understanding of the processes which occur in radiation heat transfer in participating media. For example, Stamnes and Conklin [1] investigated radiative heat transfer in vertically inhomogeneous atmospheres; Stepanov et al. [2] studied a solid slab with semi-transparent selective boundaries; Siegel [3] solved the problem of radiative exchange in a parallel-plate enclosure with translucent protective coatings.

Radiative heat transfer in two-layer systems is of great interest, since it has practical applications in crystalliza-

tion processes, various measuring and detection devices, etc. Therefore, such systems have been widely studied, either in planar or cylindrical geometry [4–8]. In these systems, there is an important role played by the modes of reflection (in particular of the interface between the two layers) and the angular dependence of the incident flux. Marchenko et al. [6] considered a Fresnel interface. They performed accurate calculations by a ray tracing method, for a non-scattering medium with selective properties that depend on the temperature and wavelength. Liu and Wu [7] also considered a Fresnel interface, between two media that are inhomogeneous, gray absorbing and isotropically scattering. The radiation flux from the source was taken as diffuse, i.e., black heater away from the two-layer system, and a cooler was taken to be located on the other boundary. They expressed the reflectivity of the cooled boundary surface as the sum of specular and diffuse parts, the former being angular dependent. In [6] the heater and cooler surfaces were assumed to be opaque, with similar reflectivities. The problem was solved for both cases of heater and cooler away from the system boundaries or touching them.

Cengel and Ozisik [9] studied the problem of an anisotropically scattering slab with angular dependent reflectivity. Abrams and Viskanta [4] considered a diffusive interface between solid and liquid phases during melting or solidification of semi-transparent crystals. They solved the problem numerically and noted the possibility of a non-monotonous temperature field in the vicinity of the interface. An interesting result obtained from the numerical analysis is that this phenomenon occurs only at the beginning of the transient melting process but not under steady conditions. In this investigation it was assumed that the semi-transparent media are in contact with opaque emitting surfaces. Aronov et al. [10] showed later that non-monotonous temperature fields can exist near a diffusely transmitting interface at steady state. This phenomenon appears when the radiation incident on the interface is primarily directed (collimated, “focused”) normal to the surface, e.g., due to angular-dependent reflectivities and emissivities of the opaque boundary surfaces. The non-monotonous behavior can be exhibited when a diffuse radiation flux from the heater is “focused” on the system boundary by Fresnel refraction. It was further observed by [10], that for media of small optical thickness the temperature field can be not only non-monotonous but also inverse: it can increase monotonously from the boundary facing the heater to that facing the cooler. This phenomenon was demonstrated in the experimental work of Aronov et al. [11] and studied analytically in [12] by the same authors. Aronov et al. [13] investigated non-monotonous stationary temperature fields

in a plane translucent layer heated by collimated radiation, in case of an “optically open” system, defined in Section 2 (see figure 1).

The studies in [2, 4–10] treated conjugate problems of conduction–radiation. Aronov et al. [13] and Lee and Pomraning [14] studied pure radiation problems. Under the effect of the conduction heat transfer mode, the phenomena described above are not (or weakly) exhibited. They have been discovered for a conjugate radiation problem, i.e., [10, 11].

It is emphasized that these phenomena of non-monotonous and inverted temperature fields have important implications: for example, in the case of solidification of optical crystals they can lead to break-down of the process or to undesired properties. Such problems (if known in advance) can be avoided by proper control of the process, e.g., dis-focusing of the radiation heat fluxes in the case described above. Other cases where the phenomena of inverted and non-monotonic temperature fields may be encountered and play important roles, are radiative transfer in an atmosphere with diffusive layers (such as dust-bearing layers), in material processing by laser beams, in preparing multi-layered optical coatings, etc.

The present paper treats, for the first time, pure heat radiation in a double-layer system with a diffuse or partially diffuse interface between them. Such an interface between two layers (or even within a homogeneous medium) appears, for example, in several situations of infringement during crystallization processes, due to plane dislocations, admixtures or bubbles. For a “closed system”, where the heater and cooler are opaque surfaces located away from the system or on its boundaries, the results obtained from the numerical analysis of the problem show a break-down (jump) of the temperature field near the diffuse or partially diffuse interface. In cases of small optical thickness, an inversion of the temperature distribution occurs. The inversion phenomenon was obtained also in [10], but with continuous temperature profiles, due to conduction. Another interesting result here is the phenomenon of “optical heat trap”, for both a single layer and two-layer “open systems” heated by a collimated radiation flux: the temperature increases with the refraction index, n , in the former case and is higher in the layer with larger n in the latter case.

2. THEORETICAL MODEL

The problem under consideration is pure radiation heat transfer in a two-layer system (of geometrical thick-

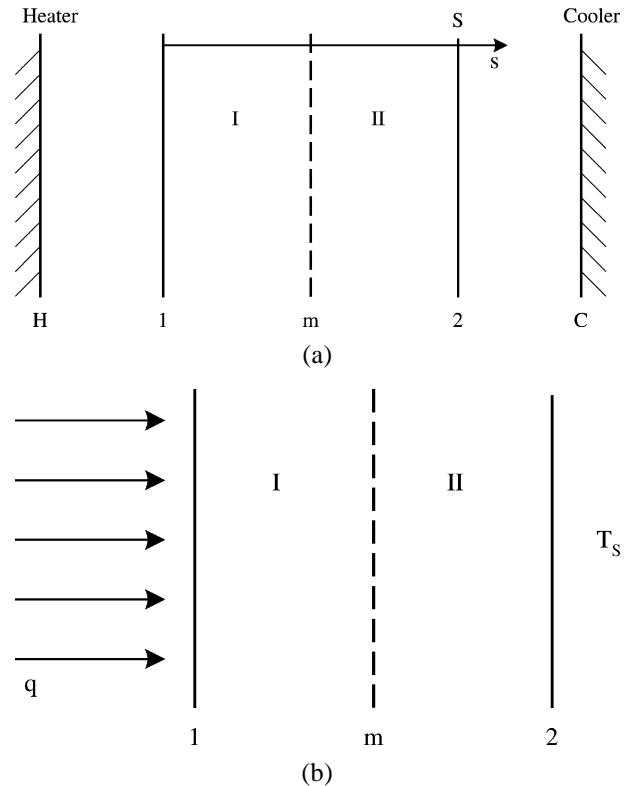


Figure 1. Schematic description of the two-layer system: (a) optically closed system; (b) optically open system.

nesses L_I and L_{II}), see figure 1. Two cases are treated: an “optically closed system”, where the layers are placed between opaque plane surfaces of heater and cooler and an “optically open” one, where the system is irradiated by a normally directed heat flux from one side, and through both the transparent boundary surfaces radiation is transmitted into space. The theoretical model is based on the following assumptions:

(1) The reflectivities, r_C , r_H , of the heater and cooler surfaces may depend on the wavelength, λ , and temperature, T , and can be expressed as the sum of specular and diffuse parts. The specular component is generally angular-dependent.

(2) The media of the layers I and II are semi-transparent (translucent). They are non-scattering, and have absorptivities, α , (equal to emissivities by Kirchhoff’s law) that may depend on the wavelength and temperature. Their refractive indices, n_I , n_{II} , may depend on λ only. In general, α and n are different in the two layers.

(3) The surroundings, including the spaces between heater/cooler and the two layers (in case of a “closed system”), have a refractive index of unity.

The equations of radiation energy transfer (RTE) in planar geometry for an emitting–absorbing non-scattering medium in thermodynamic equilibrium are written in the following form:

$$\mu \frac{\partial I_{\lambda}^{+}(s_{\lambda}, \mu)}{\partial s_{\lambda}} + \{I_{\lambda}^{+}(s_{\lambda}, \mu) - I_{b\lambda}[T(s_{\lambda})]\} = 0 \quad (1a)$$

$$\mu \frac{\partial I_{\lambda}^{-}(s_{\lambda}, \mu)}{\partial s_{\lambda}} - \{I_{\lambda}^{-}(s_{\lambda}, \mu) - I_{b\lambda}[T(s_{\lambda})]\} = 0 \quad (1b)$$

where $\mu \equiv |\cos \theta|$, θ is the polar angle of the ray and I_{λ}^{\pm} and $I_{b\lambda}$ are the integrals over the azimuth angle of the radiation intensities i_{λ}^{\pm} in the \pm directions and of $i_{b\lambda}$:

$$I_{\lambda}^{\pm} = 2\pi i_{\lambda}^{\pm} \quad (2)$$

$$I_{b\lambda}(s_{\lambda}) = 2\pi n_{\lambda}^2 i_{b\lambda}[T(s_{\lambda})] \quad (3)$$

The optical thickness, s_{λ} , is defined by:

$$s_{\lambda} = \int_0^x \alpha_{\lambda}(x') dx' \quad (4)$$

According to equation (1), $I_{\lambda}^{+}(s_{\lambda}, \mu)$ in the x -direction, can be expressed as:

$$I_{\lambda}^{+}(s_{\lambda}, \mu) = I_{\lambda}^{+}(0) e^{-s_{\lambda}/\mu} + \frac{1}{\mu} \int_0^{s_{\lambda}} I_{b\lambda}[T(s'_{\lambda})] e^{-(s_{\lambda}-s'_{\lambda})/\mu} ds'_{\lambda} \quad (5)$$

The corresponding relation for $I_{\lambda}^{-}(s_{\lambda}, \mu)$, in the opposite direction, is obtained from (5) by replacing s_{λ} by $s_{\lambda, \max} - s_{\lambda}$, where $s_{\lambda, \max}$ is the maximal optical thickness inside the relevant medium (layer). Equations (1)–(5) appear in the literature in various detailed presentations, e.g., [15–17]. Henceforth, all the intensities I without the index λ denote integrals over the wavelengths.

For the case of optically closed system, the surfaces H and C of the heater and cooler (figure 1) are opaque, with specular reflectivities r_H and r_C . Hence the boundary conditions for $I = 2\pi i$ are:

$$I_H^{+}(\mu) = I_H(\mu) + r_H I_H^{-}(\mu) \quad (6)$$

$$I_C^{-}(\mu) = I_C(\mu) + r_C I_C^{+}(\mu) \quad (7)$$

where:

$$I_j(\mu) = 2\pi i_b[1 - r_j(\mu)], \quad j = H, C \quad (8)$$

The external semi-transparent boundaries of the layers (1) and (2), (see figure 1) are taken as Fresnel surfaces. The two layers are assumed to have the same absorptivities, geometrical and optical thicknesses, but their refrac-

tion indices n_I and n_{II} are generally different. In the particular case when they are equal, the interface, m, which is diffusive or partially diffusive, separates the system such that it is still a two-layer one. Furthermore, the interface has partially diffusive and partially specular reflectivities and transmissivities. The limiting case of a single layer is also treated, serving as reference.

Normalized radiation intensities, J , for the two layers I and II are introduced by:

$$J_j = n_j^{-2} I_j, \quad j = I, II \quad (9)$$

The normalized intensities at the interface, m, are related by the following equations:

$$J_I^{-}(x_m, \mu) = K r_{s, mI}(\mu) J_I^{+}(x_m, \mu) + (1 - K) r_{d, mI} Z_I + K [1 - r_{s, mII}(\eta)] J_{II}^{-}(x_m, \eta) + (1 - K)(1 - r_{d, mII}) Z_{II} \quad (10)$$

$$J_{II}^{+}(x_m, \eta) = K r_{s, mII}(\eta) J_{II}^{-}(x_m, \eta) + (1 - K) r_{d, mII} Z_{II} + K [1 - r_{s, mI}(\mu)] J_I^{+}(x_m, \mu) + (1 - K)(1 - r_{d, mI}) Z_I \quad (11)$$

where K is the “specular fraction”, defined by the fraction of the radiation flux incident on the interface, that is reflected and refracted by it specularly, i.e., as by an optically smooth surface. The interface radiation properties are determined in the following way. At the first stage, the “purely specular” reflectivities of the interface, $R_{s, mj}$ with $j = I, II$, on its two sides facing layers I and II, respectively, are calculated by the Fresnel relationships as functions of the incident angle, θ , and the refraction indices, n_I , n_{II} . Then, for any stipulated value of K for the general case, the specular parts of the interface reflectivity are calculated by $r_{s, mj} = K R_{s, mj}$ (and similarly for the interface transmissivity). The corresponding diffuse parts of the reflectivities, $r_{d, mj}$ (hemispherical–hemispherical), are obtained from the requirement of energy conservation, i.e., $r_{d, mj} = (1 - K) \cdot 2 \int_0^1 \mu R_{s, mj} d\mu$. It is assumed, similar to [10], that they are related to one another by:

$$(1 - r_{d, mI}) n_I^2 = (1 - r_{d, mII}) n_{II}^2 \quad (12)$$

Obviously, this expression holds exactly for the case of purely diffuse interface. The angles of incidence and refraction of the ray at the interface, represented by their cosines, μ and $\eta \equiv \mu_r \equiv \cos \theta_r$, are related through Snell’s law, e.g., for a ray incident from layer I:

$$n_I^2 (1 - \mu^2) = n_{II}^2 (1 - \eta^2) \quad (13)$$

and Z_I , Z_{II} are defined by:

$$Z_I \equiv 2 \int_0^1 J_I^-(x_m, \mu') \mu' d\mu' \quad (14)$$

$$Z_{II} \equiv 2 \int_0^1 J_{II}^-(x_m, \eta') \eta' d\eta' \quad (15)$$

A semi-analytical algorithm of solving the set of equations (1)–(15) is described by [6, 10, 12], and in more detail by [16]. For the case of pure radiation heat transfer, the energy equation for a planar medium is:

$$C(T) \frac{\partial T(x)}{\partial t} = - \frac{\partial F(x, t)}{\partial x} \quad (16)$$

where $C(T)$ is volumetric specific heat. The resultant radiation flux in the x -direction, $F(x, t)$, is determined by:

$$F(x, t) = \int d\lambda \int_0^1 [I_{\lambda, \psi}^+(x, t) - I_{\lambda, \psi}^-(x, t)] \mu d\mu \quad (17)$$

Here $\psi = \mu$ for $x < x_m$ and $\psi = \eta$ for $x > x_m$. $I_{\lambda, \psi}^{\pm}(x, t)$ are the intensities multiplied by 2π , similar to $I_{\lambda}^{\pm}(s_{\lambda}, \mu)$ in equations (1) and (2), but at the time t and as a function of distance x instead of optical thickness s_{λ} .

The problem is solved by a finite differences numerical method, based on that developed and described by Aronov et al. [10]. The two-layer system is represented by control elements, and an energy balance is written for each element, including the absorption in it of radiation penetrating through the boundaries (see *figure 1*) and radiation emitted by every other element and reaching it, and the emission from this element. For each control element i , equation (16) is represented by:

$$C_i(T_i^k) \frac{T_i^{k+1} - T_i^k}{\Delta t} = - \frac{Q_i(T^k)}{x_{i+1/2} - x_{i-1/2}}, \quad i = 1, 2, \dots \quad (18)$$

where T^{k+1} is the current temperature, at time $t + \Delta t$, T^k is that at the previous time step, k , at time t , $x_{i\pm 1/2} = 0.5(x_i + x_{i\pm 1})$ and Q is defined by:

$$Q_i(T^k) = F_{i+1/2}(T^k) - F_{i-1/2}(T^k) \quad (19)$$

It is noted that F and Q are determined by the whole temperature field, T , see the definition of F in equation (17). For the control element near the left boundary of layer I, at $i = 0$, the following relation replaces equation (18):

$$C_0(T_0^k) \frac{T_0^{k+1} - T_0^k}{\Delta t} = - \frac{Q_0(T^k)}{0.5(x_1 - x_0)} \quad (20)$$

where in the equation for Q_0 :

$$\begin{aligned} x_{-1/2} &= x_0, & x_{+1/2} &= (x_1 + x_0)/2 \\ F_{-1/2} &= F_0, & F_{+1/2} &= F[(x_1 + x_0)/2] \end{aligned} \quad (21)$$

and an expression similar to (20) is written for the right boundary of layer II.

The problem under consideration here is steady state radiation, i.e., time-independent. Thus k actually means the k 's iteration in an implicit numerical scheme, and Δt is a pseudo time step. The numerical solution procedure is employed for each “time”, t^k , or iteration, k . An explicit difference scheme for the solution might be quite unstable, since the effective radiation conductivity of the semi-transparent medium can exhibit drastic increase.

Therefore, the following expansion of the Planck function for $i_{b\lambda}$ that appears in the function F is introduced:

$$i_{b\lambda}(T^{k+1}) = i_{b\lambda}(T^k) + \frac{\partial i_{b\lambda}(T)}{\partial T} (T^{k+1} - T^k) \quad (22)$$

Substitution of the last relationship into equations (17) and (19), and adopting an approximation whereby only the contributions of the neighboring elements are taken into account, the following expression for Q_i is obtained:

$$\begin{aligned} Q_i &= Q_i(T^k) - \alpha_{i-1} \alpha_i \frac{\partial Q_{i-1}^k}{\partial T_{i-1}^k} (T_{i-1}^{k+1} - T_{i-1}^k) \\ &\quad - \alpha_{i+1} \alpha_i \frac{\partial Q_{i+1}^k}{\partial T_{i+1}^k} (T_{i+1}^{k+1} - T_{i+1}^k) \\ &\quad + 2\alpha_i \frac{\partial Q_i^k}{\partial T_i^k} (T_i^{k+1} - T_i^k) \end{aligned} \quad (23)$$

where α_i is the emissivity (equal to the absorptivity) of the control element i . It is calculated as $1 - \exp(-\sigma)$, where σ is the optical thickness of the element under consideration. This so-called linearization simplification renders the numerical scheme implicit and stable, since T^{k+1} appears on the RHS of equations (18) and (19) for all the control elements. A predictor–corrector method has been used for the solution, with the Thomas algorithm, which accelerates significantly the computations for stationary problems, [18].

An equi-distance grid of elements was used for solving the equations. At the beginning of the external time loop, the divergence of the radiation flux, $\partial F / \partial x$, is obtained from equations (1)–(15) based on the temperature field from the previous iteration step. The calculation begins with an initial guess for the temperature field (“zero approximation”). The predictor–corrector method

TABLE I

Effect of the grid size on the temperature profile, $T(s/S)$.
 M is the number of control elements. Optically closed system: diffuse interface, $K = 0$; $S = 0.75$. $\alpha_H = \alpha_C = 1$; $n_I = n_{II} = 1.1$.

s/S	$T(K)$		
	$M = 20$	$M = 40$	$M = 80$
0.4	841.80	841.76	841.73
0.4125			839.84
0.425		837.91	837.88
0.4375			835.82
0.45	833.80	833.71	833.66
0.4625			831.39
0.475		829.04	828.97
0.4875			826.39
0.5125			854.69
0.525		852.27	852.33
0.5375			850.09
0.55	847.81	847.90	847.95
0.5625			845.88
0.575		843.85	843.88
0.5875			841.95
0.6	839.99	840.03	840.06

is very efficient, and provides rapid convergence of the solution, irrespective of the choice of “zero approximation”. Therefore, for example, a uniform temperature profile can be taken, with $T^4 = (T_H^4 + T_C^4)/2$.

In all the computations performed for the results presented here, the number of control elements was 20. The accuracy provided by the method is demonstrated in *table I*, showing an example for the effect of the grid size on the convergence of the temperature profiles. As can be seen, there are very slight differences—fractions of degree only—between the values of T at the same nodes, when the number of control elements was increased from $M = 20$ to 80. The integrals over every interval of μ or η were performed by 3 or 5 point Gaussian quadratures, depending on the interval size (after checking convergence by comparisons with results obtained by 5 and 7 point quadratures) and the value of the pseudo time step was taken as 10^5 s (very large, showing the stability of the solution procedure). A full relaxation of the temperature field was generally obtained at less than 30 iterations.

3. RESULTS AND DISCUSSION

The solution procedure and algorithm described in the previous section have been applied for solving the prob-

lem of pure radiation heat transfer in the two-layer system shown in *figure 1*. The media are semi-transparent and the interface between the layers has reflectivity and transmissivity which are partially specular and partially diffuse. A parametric study has been performed for assessing the influence of various effects and radiation properties on the behavior of the temperature and heat flux fields. In the following four sections, “optically closed” systems are discussed, and in the subsequent two sections—“optically open” systems are treated. Two important results, that have been found from the analysis and parametric study, are inversion of the temperature profile and temperature jump at the interface. These phenomena are due to three mechanisms causing collimation (“focusing”) of the radiation: angular dependence of the reflectivities and emissivities of the opaque boundary surfaces; Fresnel refraction; and absorption of isotropic radiation at large polar angles. Most of the cases investigated and described hereafter are for “optically closed systems” with a diffuse or partially diffuse interface (Sections 3.1–3.4), since these are directly associated with the three collimation mechanisms. These effects are more pronounced in optically closed systems. A third important result is the radiation heat trap effect, caused by total internal reflection, which is displayed more significantly for “optically open systems” with a specular interface. These systems are discussed in Sections 3.5–3.6.

The algorithm described above was developed for non-gray radiation problems, where the radiation properties may depend on the wavelength and on the temperature. In general, these problems, having spectral (or selective) properties, are certainly not linear. However, in all the cases considered here for the parametric study of the effects mentioned above, the radiation properties, which determine each case, were taken as constant. Hence, for these cases the model results are linear in the fourth degree of the temperatures. Therefore, the computations were performed, for simplicity, with single values of the heater and the cooler temperatures, $T_H = 1000$ K, $T_C = 1$ K for optically closed systems; and with several values of the incident heat flux q , that are convenient for various comparisons, for open systems in a cold space, $T_s = 0$ K. Under these conditions, multiplying T_H by a factor b , or the incident heat flux by a factor b^4 , lead to multiplication of the corresponding temperature profiles by b .

The procedure was validated quantitatively, by comparison with available results, for the two cases of two-layer system with small optical thickness and diffuse interface—[10]; and one-layer semi-transparent system—[2]. It was also validated qualitatively by comparison

with [4], for the case of diffuse interface under conditions of radiative–conductive heat transfer.

3.1. Optically closed systems—effects of the interface specular fraction and the system optical thickness

Figures 2–4 show results for the temperature field for collimated radiation at the opaque surfaces of the heater and cooler (closed system). The surface emissivities depend on the polar angle, θ . In figures 2 and 3, $\alpha_H = \alpha_C = 1$ for $\mu = \cos\theta > 0.5$ and $\alpha_H = \alpha_C = 10^{-4}$ for other μ . This means that the radiation is mainly concentrated near the normal to the surfaces. Figure 2 illustrates the effect of the specular reflection factor of the interface. One curve in the figure corresponds to the case of specular interface, i.e., $K = 1$. It is noted that since in figures 2–4 the refraction coefficients of the layers are both equal to unity, $n_I = n_{II} = 1$, $K = 1$ means absence of interface: a single-layer system. In this case the temperature profile, $T(x)$, is “ordinary” or “regular”—it decreases monotonously, without any break-down, from the side facing the heater to that facing the cooler. For other values of K , a break-down of the temperature field occurs, with an inversion at the interface: T decreases from the side facing the heater to a value T_m^- near the interface, then exhibits a sharp rise to $T_m^+ > T_m^-$ and

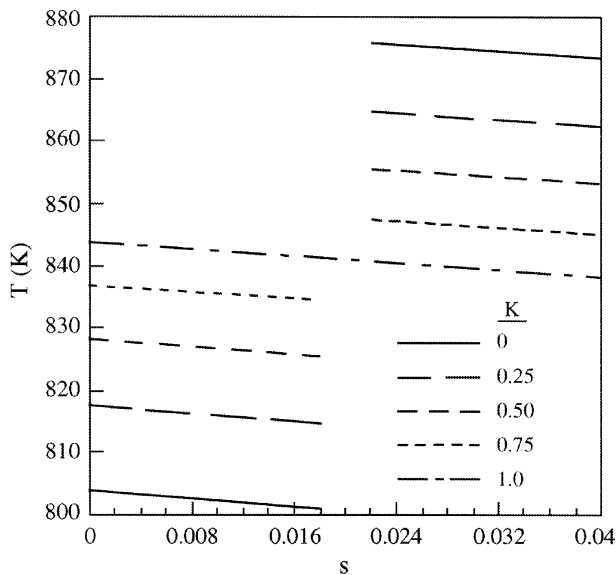


Figure 2. Temperature distribution, $T(x)$ —effect of the interface specular reflection fraction, K . Optically closed system; $n_I = n_{II} = 1$; $S = 0.04$; $\alpha_H = \alpha_C = 1$ for $\cos\theta \geq 0.5$ and 10^{-4} for other θ ; $T_H = 1000$ K, $T_C = 1$ K.

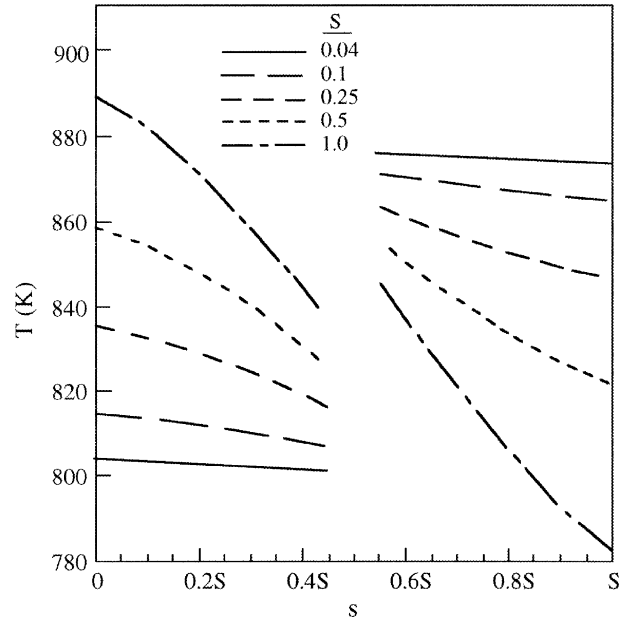


Figure 3. Temperature distribution, $T(x)$ —effect of system optical thickness, S . Optically closed system; diffuse interface, $K = 0$; other parameters as in figure 2: $n_I = n_{II} = 1$; $\alpha_H = \alpha_C = 1$ for $\cos\theta \geq 0.5$ and 10^{-4} for other θ ; $T_H = 1000$ K, $T_C = 1$ K.

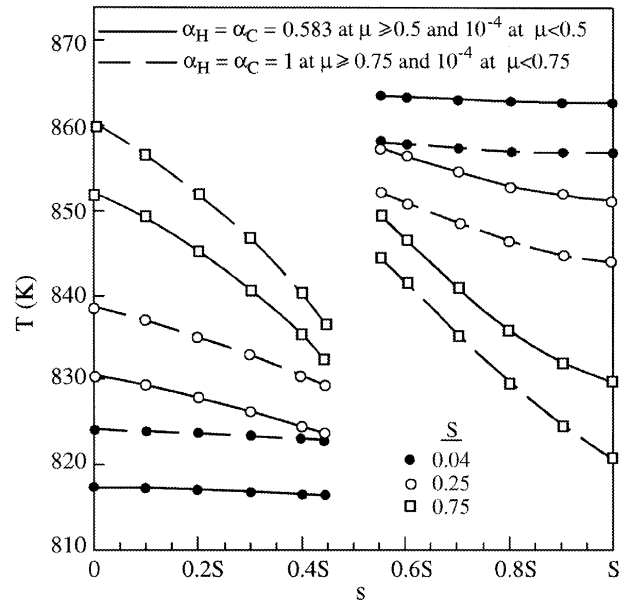


Figure 4. Temperature distribution, $T(x)$ —effects of optical thickness, S , and of degree of collimation. Optically closed system; diffuse interface, $K = 0$; other parameters as in figure 2: $n_I = n_{II} = 1$; $T_H = 1000$ K, $T_C = 1$ K.

then decreases, again, to the side facing the cooler. This phenomenon is also observed in *figure 3*, where $T(x)$ is plotted for various values of the optical thickness of the two-layer system, S . However, another interesting phenomenon is seen here: for a system which is relatively optically thin (small S), the entire temperature curve in layer I, facing the heater, lies below that in layer II, facing the cooler.

These two phenomena are explained as follows. For collimated radiation (near normal) and specular interface, most of the rays travel relatively short distances. When the diffuse part of the reflectivity increases, more transmitted diffusely rays are directed at larger angles in layer II, with longer paths, resulting in more absorption. The effect is obviously stronger when the system is optically thin, and when the specular reflection part of the interface is smaller. In addition, a considerable part of the intrinsic emission from the relatively thin layer II is radiated by grazing rays. These are scattered at the partially diffuse interface and then travel shorter distances in layer I, with less absorption of energy than in the specular case.

The effect of collimating (“concentrating”) the heat flux radiated by the heater and cooler surfaces is illustrated in *figure 4*. The dashed line represents higher degree of concentration (larger emissivity at a narrower angle range). It is clearly seen that the two phenomena discussed above, inversion and break-down of the temperature field, become more pronounced as the radiation of the same integral value is more collimated.

The phenomenon of temperature field inversion is similar to that found by Aronov et al., [10]. However, the problem that they analyzed was combined radiation and conduction, and therefore without the break-down in the temperature distribution.

3.2. Optically closed systems—effects of focusing by Fresnel refraction at the boundaries

The cases, which have been treated previously, were for layers having refraction index of unity. In the following, the effects of Fresnel “focusing” (collimating), caused by different values of $n_I = n_{II}$ are investigated (the space between the two layers and heater/cooler has $n = 1$). *Figure 5* shows the behavior of the temperature field for several values of $n = n_I = n_{II}$, for diffuse interface ($K = 0$) and system optical thickness $S = 0.75$. The two phenomena observed and discussed above are clearly depicted, again: the temperature field break-down at the interface and the inversion of the T -profile, with higher

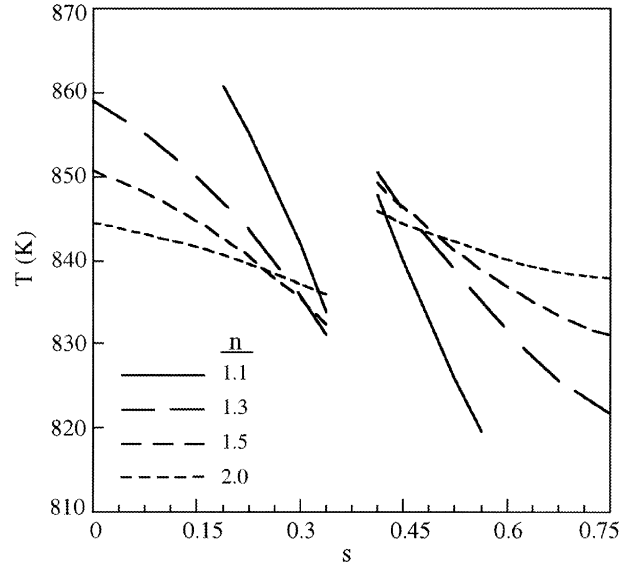


Figure 5. Temperature distribution for isotropic radiation, $T(x)$ —effect of Fresnel collimation, various values of the refraction index, $n = n_I = n_{II}$. Optically closed system; diffuse interface, $K = 0$; $S = 0.75$; $\alpha_H = \alpha_C = 1$; other parameters as in *figure 2*: $T_H = 1000$ K, $T_C = 1$ K.

TABLE II
Maximal temperature jump at the interface (inverted T -field) at associated values of the refraction index $n = n_I = n_{II}$ as a function of the optical thickness, S . Optically closed system; diffuse interface, $K = 0$; Fresnel collimation of isotropic radiation by heater and cooler, $\alpha_H = \alpha_C = 1$.

$n = n_I = n_{II}$	1.1	1.15	1.25
S	0.04	0.25	0.75
ΔT_{\max} (K)	74.8	46.7	19.5

temperatures in the layer facing the cooler than in that facing the heater. Another interesting phenomenon has been found here: the temperature jump at the interface, ΔT_m , is not a monotonous function of the refraction index, n . As can be seen, in the range $1 < n < 2$, ΔT_m attains a maximum value at $n \approx 1.3$. This phenomenon is explained by the influence of multiple reflections at the system semi-transparent boundaries. The effect of the optical thickness, S , is shown in *table II*, which includes the maximum value of the temperature jump, ΔT_{\max} , at the associated values of the refraction index, n , for diffuse interface. As can be seen, as the system becomes optically thinner (smaller S), ΔT_{\max} increases and is obtained at smaller n .

It is noted that the temperature distributions presented in *figures 2–6*, *8* and *9* have been obtained by the

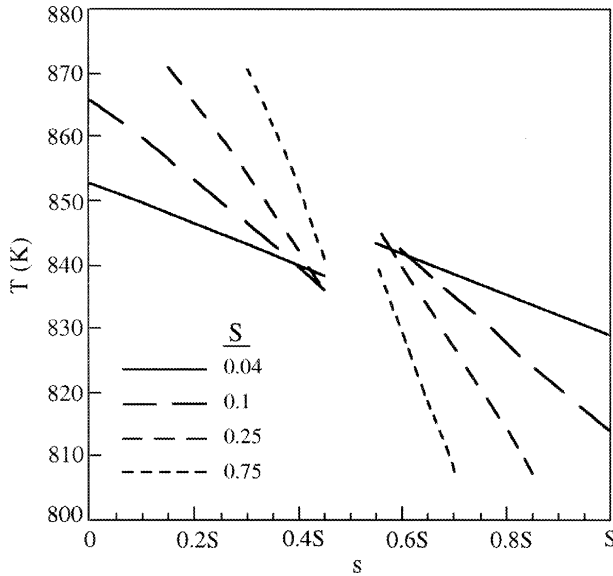


Figure 6. Temperature distribution for isotropic radiation, $T(x)$ —effect of system optical thickness, S . Optically closed system; diffuse interface, $K = 0$; $n_I = n_{II} = 1$; other parameters as in figure 5: $\alpha_H = \alpha_C = 1$; $T_H = 1000$ K, $T_C = 1$ K.

TABLE III

Temperature jump at the interface (inverted T -field), $\Delta T_m(K)$ —effects of $n_{II} > n_I = 1$, and of collimation pattern. Optically closed system; diffuse interface, $K = 0$; $S = 0.04$. Case (a): $\alpha_H = \alpha_C = 1$ for $\cos \theta \geq 0.75$ and $\alpha_H = \alpha_C = 10^{-4}$ for other θ . Case (b): $\alpha_H = \alpha_C = 0.583$ for $\cos \theta \geq 0.5$ and $\alpha_H = \alpha_C = 10^{-4}$ for other θ .

n_{II}	1.1	1.2	1.25	1.3	1.35
(a)	27.9	15.2	10.1	5.7	1.8
(b)	19.6	8.3	3.8		

In case (b), no temperature jump at the interface has been observed for $n \geq 1.28$.

TABLE IV

Temperature jump at the interface (inverted T -field)—effect of optical thickness. Optically closed system; diffuse interface, $K = 0$; $n_I = n_{II} = 1$; $\alpha_H = \alpha_C = 1$.

S	0.04	0.10	0.25	0.50	0.75
$\Delta T_m(K)$	5.4	9.5	10.5	5.4	0

numerical code after it was seen that sufficient conversion is reached by a grid of 20–40 nodes. Thus the values of T_m^- and T_m^+ near the interface are those obtained in the centers of the corresponding control elements. It was also observed that these temperatures smoothly approach finite values at the interface when the grid size is made smaller and smaller, as demonstrated above, see table I. Therefore, the temperature jumps, ΔT_m , presented in tables II–IV, were obtained by simple extrapolations.

Table III shows the dependence of ΔT_m on n_{II} , for $n_I = 1$, and of the heater and cooler emissivities and of their angular behavior. As could be expected, ΔT_m is higher, again, when the heater and cooler surfaces are more collimating (case (a)), and also for smaller n_{II} .

3.3. Optically closed system—effect of absorption of isotropic radiation at large polar angles

In all the cases studied above, the phenomena of break-down and inversion of the temperature field were observed to occur due to collimation of the radiation by angular-dependent properties of the heater and cooler surfaces or by Fresnel collimation (n_I and/or n_{II} not equal to unity). As can be seen in figure 6, the former phenomenon is also exhibited for isotropic radiation emitted by the heater/cooler, when $\alpha_H = \alpha_C = 1$ and for $n_I = n_{II} = 1$ (without Fresnel collimation). The reason for this behavior is the following: in this case (unlike the previous cases), there is a substantial part of incident radiation beams that travel at rather large polar angles, and their optical path in layer I is therefore larger and the absorption is stronger. The radiation incident on the diffuse interface becomes collimated since there are less grazing beams originated in the isotropic radiation.

Table IV includes the values of temperature jumps at the interface, for several values of the system optical thickness. Obviously, the influence of absorption of isotropic radiation, considered here, is weaker than the effects studied above of K , S , and of collimation by angle-dependent α_H , α_C and by n_I , $n_{II} \neq 1$.

3.4. Optically closed systems—effects of the refraction index and optical thickness on the radiation heat fluxes

Figure 7 (a) and (b) show the dependence of the radiation flux, q , on the refraction index $n = n_I = n_{II}$ for various values of the optical thickness, S , at $\alpha_H = \alpha_C = 1$. The case of diffuse interface, $K = 0$, is presented in figure 7(a) and that of specular interface, $K = 1$, in figure 7(b). The latter actually corresponds to a one-layer system, since the optical properties are identical in the two layers of the system under discussion.

As can be seen from both figures, the heat flux diminishes when the optical thickness increases. This is obviously caused by the decrease of the system transmis-

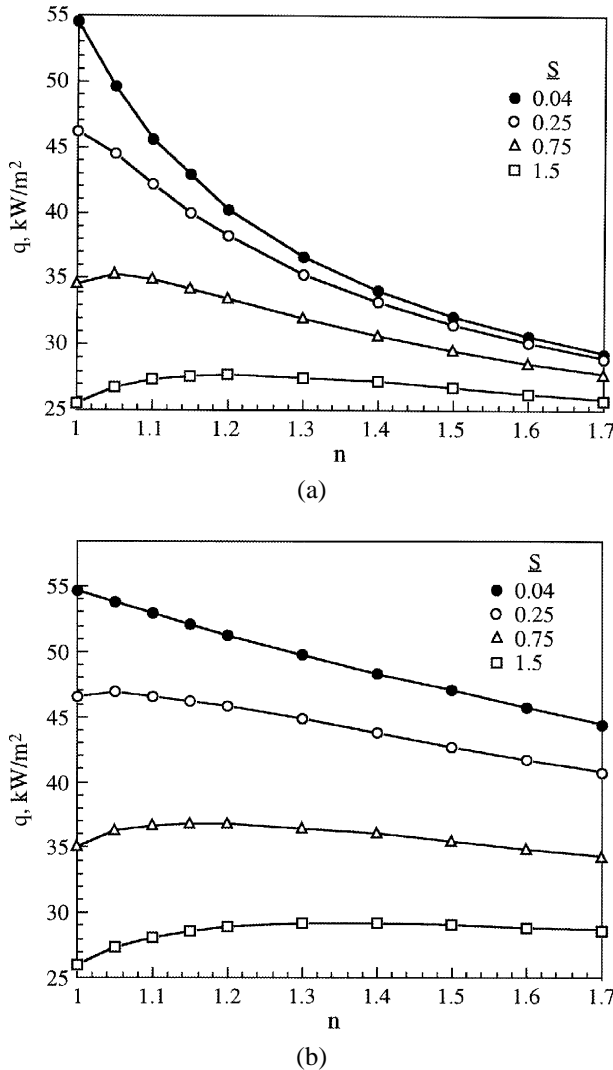


Figure 7. Radiation flux, q , as a function of the refractive index $n = n_I = n_{II}$ —effect of the system optical thickness, S . Optically closed system; $\alpha_H = \alpha_C = 1$; $T_H = 1000$ K, $T_C = 1$ K. (a) Diffuse interface, $K = 0$; (b) Specular interface, $K = 1$.

sivity with increasing S . The effect of the refractive index is more complicated: on one hand, the system transmissivity is lower for larger n due to the growth of its reflectivity. On the other hand, Fresnel refraction collimates the radiation flux, diminishing its absorption and increasing the system transmissivity. Therefore, the function $q(n)$ has a maximum for relatively large S , where the collimation effect is more significant. For the cases shown in figure 7(a), the radiation flux is focused, by Fresnel refraction, in the first layer (facing the heater),

and then scattered by the diffuse interface. The results in figure 7(b) for specular interface (where the focusing effect is more pronounced) show, indeed, that the $q(n)$ function exhibits a maximum at smaller values of S than for the case of diffuse interface, figure 7(a). The maximum of q is attained at lower values of n in the case of $K = 0$ (figure 7(a)) than for $K = 1$ (figure 7(b)), and the slopes of the $q(n)$ curves are more moderate in the latter case of $K = 1$.

3.5. Optically open system—specular interface, heat trap effect

For “optically open” systems (see figure 1), only the case of collimated radiation is considered, e.g. the primordial radiation flux incident on the boundary surface 1 is collimated (uni-directional). In order to facilitate comparisons of various cases, it is necessary to define the set of input parameters to serve as a “common denominator”. Thus for open systems, a uni-directional heat flux incident on the boundary, q , was selected in the following way. For a thin one-layer open system with refraction index $n = \max(n_I, n_{II})$, q will produce the same value of the interface temperature, T_m , as for an identical medium between opaque boundaries (optically closed system) with $\alpha = \alpha_H = \alpha_C = 1 - r$. It is known that for this case, $T_m = [0.5(T_H^4 + T_C^4)]^{1/4}$ and for $T_H \gg T_C$, $T_m \approx \sqrt[4]{0.5} T_H$.

For optically open systems it has been found that the phenomena of temperature field break-down and inversion are exhibited even for specular interface. This happens when the refraction index of the layer facing the cooler is larger than that facing the heater, $n_{II} > n_I$. The results in figure 8 show the behavior of the temperature distribution for various values of n_{II} , for $n_I = 1$, $K = 1$ and $S = 0.04$. Here the inversion is not the result of focusing the radiation flux, since the specular interface changes the degree of collimation in the opposite direction, impeding the inversion. It was also found that when $n_I > n_{II}$, the T -distribution is not inverted, and the temperature in the layer facing the heater is higher. Thus the effect of inversion observed in figure 8 for $n_I < n_{II}$ is explained by total interior reflection at the corresponding incident angles, which is more pronounced in the layer with larger n . Table V includes results for the heat flux calculated as indicated above, for a one-layer system with the stipulated T_m . As can be seen, q diminishes with increasing refraction index.

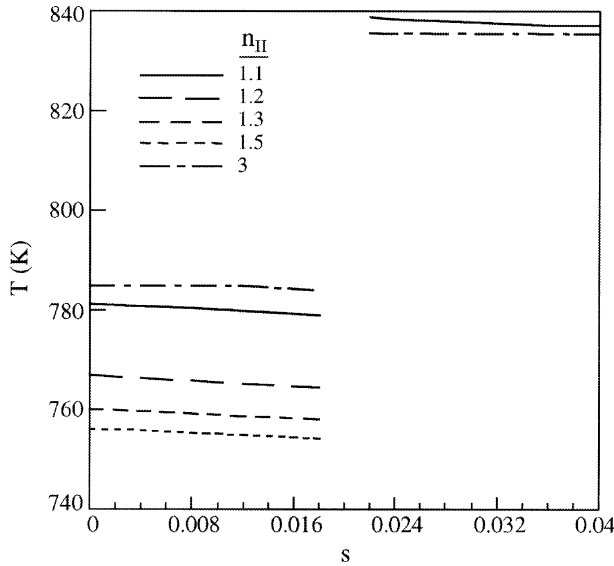


Figure 8. Temperature distribution, $T(x)$ —effect of the refraction index n_{II} . Optically open system; specular interface, $K = 1$; $n_I = 1$; $S = 0.04$; $T_s = 0$ K; the incident heat flux, q , is such that $T_m \approx \sqrt[4]{0.5T_H}$ as for a closed system with heater and cooler having the same optical properties and $T_H = 1000$ K, $T_C = 0$ K. The curves for $n_{II} = 1.2, 1.3, 1.5$ in layer II lie between those for $n_{II} = 1.1, 3$.

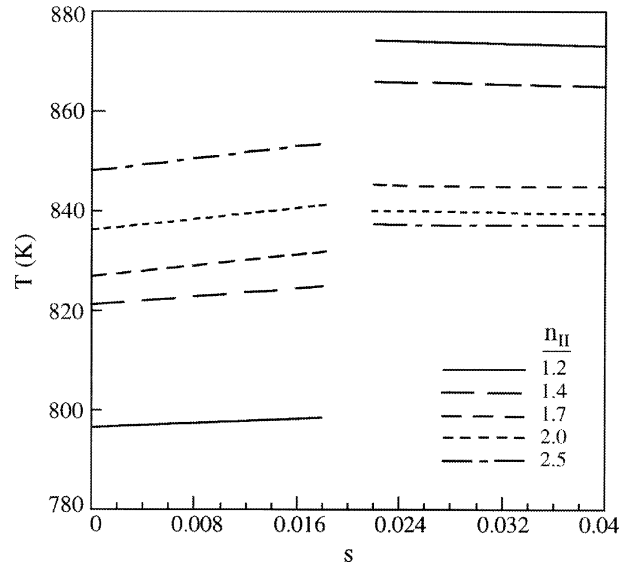


Figure 9. Temperature distribution $T(x)$ —effect of the refraction index n_{II} ; optically open system; diffuse interface, $K = 0$; other parameters as in figure 8: $S = 0.04$; $T_s = 0$ K; the incident heat flux, q , is such that $T_m \approx \sqrt[4]{0.5T_H}$ as for a closed system with heater and cooler having the same optical properties and $T_H = 1000$ K, $T_C = 0$ K.

TABLE V

Collimated radiation flux, q that yields
 $T_m \approx \sqrt[4]{0.5} \times 1000$ K—effect of the refraction index, n .
 Optically open one-layer system with optical thickness
 $S = 0.04$.

n	1	1.1	1.2	1.3	1.5	1.8	2.0	3.0
q (kW·m ⁻²)	107.2	78.4	71.9	68.3	64.3	61.4	60.3	58.1

3.6. Optically open system—diffuse interface

Figure 9 shows the behavior of the temperature distribution for a two-layer open system with a diffuse interface, $K = 0$, for $n_I = 1$, $S = 0.04$ and various values of n_{II} . In this case, the inversion of the temperature field is exhibited only for relatively small values of n_{II} , while for n_{II} values larger than about 1.9 the temperature profile behaves “regularly”. An interesting phenomenon obtained here, in contrast to the results seen above, is the monotonous increase of the temperature in the layer facing the heater. This phenomenon is not associated with the interface properties only. It is known that collimated radiation can produce a temperature increase or a temperature decrease with depth, depending on the incidence angle. For example, the former corresponds to normal in-

cidence. The behavior of the systems under consideration here and the effects studied are the results of all the system parameters, including the interface and layers properties (refraction index and optical thickness) and the direction of the collimated incident flux.

4. SUMMARY

A theoretical method and numerical algorithm were developed to describe pure radiation heat transfer in a two-layer system of media that are non-scattering and semi-transparent. The method has been applied to study various effects of the optical (radiative) properties of the media, the interface and opaque surfaces of heater and cooler enclosing the layers in case of “optically closed” system. An “optically open” system has also been investigated, where the system is irradiated by a constant normal heat flux. In both cases the external boundaries of the layers are transparent Fresnel surfaces.

Stationary temperature distributions have been obtained, which exhibit break-down at the interface and inversion, in case of diffuse or partially diffuse interface. A maximal temperature jump occurs at vanishing interface reflection, ($n_I = n_{II}$), i.e., diffuse transmittance. For systems with relatively small optical thickness, the entire

temperature curve in the layer facing the heater (or the incident heat flux) lies below that in the other layer (facing the cooler). This phenomenon is explained by the change in direction of the rays. They are collimated into the first layer as a result of the angular-dependent emissivity of the heater and/or by Fresnel refraction, and by primary absorption of grazing rays in the first layer. Then they travel along rather short optical paths through it, and are “de-focused” at the diffuse (or partially diffuse) interface into the second layer. This causes larger optical paths in the second layer, resulting in more absorption. Furthermore, a considerable part of the intrinsic emission in the relatively thin layer II is radiated by rays at grazing angles. These are scattered at the interface and then travel shorter distances in layer I with less absorption than in the specular case.

For optically open systems the phenomena of breakdown and inversion of the temperature field are exhibited even for a specular interface. These phenomena can occur only when $n_I < n_{II}$, while for $n_I > n_{II}$ layer I is hotter than layer II (the temperature curve is higher in the former than in the latter). This effect is explained by total internal reflection at the corresponding incident angles, which is more pronounced in the layer with larger n . It has also been shown that for a one-layer open system, when n increases, a smaller incident heat flux produces the same temperature field. This is the “heat trap” effect, resulting from increased heat absorption at larger n .

Acknowledgement

The research work described in this paper has been sponsored by the Berman–Shein Mexico Energy Research Foundation, and by the Center for Absorption in Science of the Israeli Ministry of Absorption, whose support is greatly appreciated by the authors.

REFERENCES

- [1] Stamnes K., Conklin P., A new multi-layer Discrete Ordinate approach to radiative transfer in vertically inhomogeneous atmospheres, *J. Quant. Spectrosc. Rad. Trans.* 31 (1984) 273–282.
- [2] Stepanov S.V., Petrov V.A., Bityukov V.K., Radiative-conductive heat transfer of a selective medium with semitransparent boundaries, *High Temperatures (USA)* 16 (1978) 1091–1098.
- [3] Siegel R., Radiative exchange in parallel-plate enclosure with translucent protective coatings on its walls, *Internat. J. Heat Mass Transfer* 42 (1999) 73–84.
- [4] Abrams M., Viskanta R., The effect of radiative heat transfer upon the melting and solidification of semitransparent crystals, *J. Heat Transfer* 96 (1974) 184–190.
- [5] Ozisik M.N., Shouman S.M., Source function expansion method for radiative transfer in a two-layer slab, *J. Quant. Spectrosc. Rad. Trans.* 24 (1980) 441–449.
- [6] Marchenko N.V., Aronov B.I., Shtipelman Ya.I., The Stefan problem for combined radiative and conductive heat transfer in a plane layer of a selective semitransparent medium, *High Temperatures (USA)* 20 (1982) 728–736; translation of: *Teplofiz. Vys. Temp. (USSR)* 20 (1982) 897–906.
- [7] Liou B.T., Wu C.Y., Composite discrete ordinate solutions for radiative transfer in a two-layer medium with Fresnel interfaces, *Numer. Heat Transfer A* 30 (1996) 739–751.
- [8] Wu C.Y., Wu S.C., Radiative transfer in a two-layer medium on a cylinder, *Internat. J. Heat Mass Transfer* 36 (1993) 1147–1158.
- [9] Cengel Y.A., Ozisik M.N., Radiation transfer in an anisotropically scattering slab with directional dependent reflectivities, *ASME paper* 86-HYT-28, 1986.
- [10] Aronov B.I., Lingart Yu.K., Marchenko N.V., Non-monotonic temperature fields in radiative-conductive heat transfer, *High Temperatures (USA)* 22 (1984) 101–107; translation of: *Teplofiz. Vys. Temp. (USSR)* 22 (1984) 111–117.
- [11] Aronov B.I., Lingart Yu.K., Marchenko N.V., Inversion of temperature field in leykosappire, *Teplofiz. Vys. Temp. (USSR)* 25 (1987) 191–193.
- [12] Aronov B.I., Lingart Yu.K., Marchenko N.V., Inversion of stationary temperature field of a translucent plane layer, *High Temperatures (USA)* 27 (1989) 585–592; translation of: *Teplofiz. Vys. Temp. (USSR)* 27 (1989) 737–744.
- [13] Aronov B.I., Lingart Yu.K., Marchenko N.V., Stepanov S.V., Nonmonotonic stationary temperature fields in a plane translucent layer during heating by collimated radiation, *High Temperatures (USA)* 29 (1991) 130–134; translation of: *Teplofiz. Vys. Temp. (USSR)* 29 (1991) 139–143.
- [14] Lee C.K.B., Pomraning G.C., The surface cooling effect in radiation transfer, *J. Quant. Spectrosc. Rad. Trans.* 28 (1982) 21–27.
- [15] Siegel R., Howell J.R., *Thermal Radiation Heat Transfer*, 3rd edn., Hemisphere, Washington, DC, 1992.
- [16] Petrov V.A., Marchenko N.V., *Energy Transport in Translucent Solids*, Nauka, Moscow (USSR), 1985 (in Russian).
- [17] Siegel R., Transient thermal effects of radiation energy in translucent materials, *J. Heat Transfer* 120 (1998) 4–23.
- [18] Von Rosenberg D.U., *Methods for the Numerical Solution of Partial Differential Equations*, American Elsevier, New York, 1969.